Environmental Technology & Innovation 19 (2020) 100921

Contents lists available at ScienceDirect

Environmental Technology & Innovation

journal homepage: www.elsevier.com/locate/eti

Adsorption of 3-Aminopyridine (3AP) from aqueous solution using sugarcane bagasse activated carbon (SBAC)

Gaurav B. Daware, Parag R. Gogate *

Department of Chemical Engineering, ICT, Mumbai 400019, India

ARTICLE INFO

Article history:
Received 31 December 2019
Received in revised form 22 May 2020
Accepted 23 May 2020
Available online 25 May 2020

Keywords:
Adsorption
3-Aminopyridine
Sugarcane bagasse
Kinetics
Adsorption isotherms
Column operation

ABSTRACT

Adsorption of 3-Aminopyridine (3AP) from simulated effluent using sugarcane bagasse activated carbon (SBAC) was studied based on batch and continuous operations. Characterization of synthesized SBAC was performed initially using BET and SEM analysis. Different batch experiments were performed to understand the effect of operating parameters such as initial concentration, pH, SBAC dose, time and temperature to understand the effect on the extent of adsorption. The maximum adsorption capacity for batch adsorption was established as 54.4 mg/g whereas the maximum extent of removal was 97.6 % under optimized conditions. The observed data at equilibrium was found to be best fitted to Freundlich and Langmuir adsorption isotherms. Kinetic study revealed that pseudo-second order mechanism prevailed. Desorption of 3AP using ethanol showed good reuse efficacy for five cycles. Column adsorption experiments were also performed under varying SBAC bed height, concentration of 3AP and volumetric flow rate of 3AP solution to determine the breakthrough parameters. The fitting of the Yoon–Nelson and Thomas adsorption models to the obtained breakthrough data was studied and found to be satisfactory. Maximum adsorption capacity of SBAC for adsorption of 3AP in continuous operation was established as 65.6 mg/g. The obtained results demonstrated very good performance of SBAC for effective removal of 3AP in both batch and column operations.

1. Introduction

Hazardous effects of toxic chemicals including the emerging contaminants such as pyridine derivatives are well known and the interest in developing efficient newer approaches for treatment of wastewater containing these compounds has been increasing. Various industries can release different hazardous compounds to environment through inefficiently treated wastewater, as the treatment efficacies of the applied conventional approaches may not be good to tackle emerging contaminants (Jain et al., 2004). Pyridine and its derivatives are heterocyclic aromatic compounds, typically rated as highly hazardous both for the environment and human beings by the United states Environmental Protection Agency [USEPA] (Daware and Gogate, 2020). Pyridine and its derivatives have unpleasant and pungent odour and are generally volatile in nature (Lataye et al., 2006). Pyridine and its derivatives also offer significant hazard to human health as they can be harmful to kidney, eyes, liver and nervous system (Daware et al., 2014) as well as can cause cancer on prolonged exposure.

Many pyridine derivatives are used as intermediate in agricultural industries, solvents in paint industries and as raw material in textiles, polymer, pharmaceuticals and colourant industries (Padoley et al., 2011). There is a high chance of

* Corresponding author.
E-mail address: pr.gogate@ictmumbai.edu.in (P.R. Gogate).

https://doi.org/10.1016/j.eti.2020.100921
2352-1864/

presence of pyridine derivatives in the wastewaters and indeed reports indicate that the concentrations of pyridine in the wastewater from different industries vary from 20 to 300 mg/L (Alonso-Davila et al., 2012), though the maximum allowable concentration for pyridine and its derivatives in treated wastewater is 5 mg/L (Reddy and Reddy, 2012). In the emergency period, like the spills, concentration of pyridine in the wastewater increases to a higher level. As the high levels of concentrations in wastewater relates to significant hazardous effects, it becomes crucial to develop efficient treatment strategies for treatment of wastewater consisting of any pyridine derivatives.

The various approaches reported for treating wastewater containing pyridine and its derivatives include adsorption (Mohan et al., 2005; Lataye et al., 2006), biological oxidation (Bai et al., 2009), microwave induced oxidation (Zalat and Elsayed, 2013), microbial degradation in fuel cell (Zhang et al., 2009), ultrasound induced oxidative degradation (Elsayed, 2015), photo-Fenton oxidation (Bag et al., 2009), photocatalytic oxidation in the presence of TiO_2 (Zhao et al., 2004) and ozonation (Stern et al., 1997). Even though there have been some success using these advanced methods, there are associated problems like production of toxic intermediates, much longer treatment times, higher costs of operation and problems with efficient scale up methodologies. For example, a study for degradation of pyridine reported by Elsayed (2015) based on the use of ultrasound reported maximum removal as only 53%. Zhang et al. (2009) studied the microbial degradation of pyridine solution using fuel cells and reported that 24 h are required for obtaining 95.1% removal. It was also reported that the operational cost is higher due to the use of glucose and specific enzymes. Similarly, conventional approach of biological oxidation (Bai et al., 2009) was also reported to require large treatment time of about 50 h for reaching the required treatment efficacy as required by the discharge standards. Use of advanced oxidation processes (AOP) like photocatalytic oxidation also require higher treatment costs and problems for scale up in terms of lack of efficient designs for large scale operation (Bag et al., 2009; Zhao et al., 2004). Another disadvantage of the AOP is the production of toxic intermediates. Considering these problems with the reported methods, the present work focused on simpler method of treatment as adsorption using low cost adsorbents. The work deals with synthesis of adsorbent based on acid activation, subsequent characterization for getting fundamental insights into the governing mechanisms and finally, applying the same for removal of 3-Aminopyridine (3AP) which is one of the important derivatives of pyridine.

3AP (chemical formula as $C_5H_6N_2$ and molar mass = 94.12 g/mol) is used as intermediate chemical for production of pharmaceutical drugs, plant growth regulators and hair dyes. It has colourless to pale yellow appearance and has a boiling point of 248 °C. 3AP is very harmful to living organisms as it has tendency to absorb through skin and destructive to the tissues of mucous membranes. It is also harmful to respiratory system and eyes (Karale et al., 2014). The density of 3AP is 1.107 g/L and it is highly soluble in ethanol and water. Overall it can be said that based on the facts that 3AP is very harmful, hazardous and freely soluble in water, the development of methods for efficient removal from industrial wastewater is very important. In the case of adsorption, which is a simpler option to treat 3AP containing wastewater, the application of activated carbon available commercially increases the cost of treatment. If adsorbents obtained from sustainable materials are used instead of commercial materials, the cost for treatment is expected to be lower. The current work has focused on one such sustainable material, sugarcane bagasse, which is a waste material easily obtained from sugar industry. Sugarcane bagasse offers as a low cost sustainable adsorbent and when applied commercially, this can also solve the problems of environmental pollution due to effective utilization of the bagasse. Indeed, sugarcane bagasse activated carbon (SBAC) has been reported to offer excellent adsorption characteristics for treatment of dyes (Amin, 2008) and heavy metals (Anoop and Anirudhan, 2002) etc. though no work has been performed for the removal of any of the pyridine derivatives. For removal of pyridine derivatives, though some forms of activated carbon has been applied, there have not been any studies related to the use of column operation. Literature analysis revealed 3AP removal was mainly based on the use of metal based adsorbents. Alam and Kamaluddin (2000a) investigated the adsorptive removal of 3AP using chromium ferrocyanides and manganese ferrocyanide. It was reported that the maximum amount of 3AP adsorbed was 42.2 mg/g and 14.8 mg/g for the use of chromium ferrocyanides and manganese ferrocyanide respectively at 27 °C, 0.1 g as adsorbent loading and pH of 7. Alam and Kamaluddin (2000b) investigated adsorption of 3AP on cobalt and nickel ferrocyanide. It was reported the maximum amount of 3AP adsorbed was 32.1 mg/g and 26.6 mg/g using nickel ferrocyanide and cobalt ferrocyanide respectively at 27 °C, 0.1 g as adsorbent loading and pH of 7.

Considering the analysis of earlier reported work for 3AP removal, it can be seen that though adsorption on metal ferrocyanides has been reported, these are not sustainable adsorbents and in this regards the use of sugarcane bagasse in the present work stands out as main novelty. In addition, the study on thermodynamic and kinetic analysis as well as regeneration of adsorbent and continuous column study has been presented in the current work. Batch experiments were also directed at arriving at the best operating conditions based on the detailed investigation into the effect of different operating parameters as initial pH, SBAC dose (w), batch time (t), temperature (T) and 3AP concentration (C_i). Thus the novelty of the current work focusing on initial batch studies over broad range of initial concentration (25 mg/L to 500 mg/L) to establish the fundamental parameters (thermodynamic, kinetic and isotherms) followed by the column studies, is clearly demonstrated. The column adsorption experiments were also performed at various conditions to calculate the breakthrough and exhaustion time. The studies related to the column operation are very important as it is likely that at commercial scale of operation, column mode of operation will be preferred.

2. Methodology

2.1. Materials

The bagasse was collected from a local sugar factory whereas the pollutant used in the study, 3-Aminopyridine [3AP, chemical Formula $C_5H_6N_2$] was procured from Sigma-Aldrich, Mumbai, India. The chemical of analytical grade was used as received from supplier.

2.2. SBAC preparation

The received bagasse was properly washed to remove dirt and then kept in sunlight for drying. Subsequently, the material was crushed into small size particles and kept in oven at 398 K for 24 h to make it moisture free. After drying, the material was kept in muffle furnace for 2 h at 773 K to get carbon. The obtained carbon was soaked in 30% H_3PO_4 solution in 1:1 ratio (ratio in terms of weight of carbon to weight of 30% H_3PO_4 solution) for a treatment time of 24h. Distilled water wash was then given to the treated sample to neutralize the solution (final pH of around 7). The obtained activated carbon was kept in the oven at 333 K for 4 h for drying (Adib et al., 2018). Finally, the dried activated carbon was sieved over the size range of 100 to 220 μm and the obtained material was used as adsorbent in the experimentation.

2.3. Batch experimental study

Initially, stock solution of 3AP with initial concentration of 1000 mg/L was prepared and then solutions of appropriate concentrations were obtained based on dilution to be used in experimentation. The batch study of 3AP adsorption on SBAC was performed in orbital shaker incubator obtained from Bio-Technics, India. During the experiment, 50 mL solution with desired concentration of 3AP was added into a conical flask of capacity 100 mL. A required quantity of SBAC was then added. The pH adjustment of the 3AP solution was performed using 0.1N H_2SO_4 or 0.1N NaOH as per the required pH value for the experiment. The experimental study was conducted at different pH, SBAC dose, time and initial concentrations and temperature to understand the effect of these parameters on the extent of adsorption at constant speed of 150 rpm maintained in the orbital shaking incubator. Samples were collected at regular time intervals and subjected to centrifugation for separation of any solid adsorbent present in the withdrawn samples. Minimum amount of sample volume required for analysis was withdrawn using a micropipette so that there is no major difference in the residual volume in the reactor.

The adsorption capacity of adsorbent at equilibrium was determined using following equation:

$$q_e = \frac{(C_i - C_e)}{w} \tag{1}$$

where, q_e(mg/g) represents the 3AP adsorbed on SBAC at equilibrium conditions, C_i is the initial concentration (mg/L) of 3AP in wastewater, C_e is the equilibrium concentration of 3AP (mg/L) in wastewater and w is the mass of SBAC per unit volume of solution (expressed in g/L).

Considering that C_t (mg/L) is the concentration of 3AP remaining in solution at time t, extent of 3AP removal was determined using following equation:

$$\text{Extent of removal}(\%) = \frac{(C_i - C_t)}{C_i} \times 100 \tag{2}$$

2.4. Column study

The continuous column experiments were performed using a column of 25 cm height and 2 cm inside diameter. SBAC was loaded between glass wool in the column which avoids SBAC loss. The experimental set-up for the column operation is schematically provided in supplementary data (Fig. S1). The solution containing 3AP was allowed to pass from the top of the column. A peristaltic pump obtained from Ravel Hiteks, India was used for the recirculation of aqueous solution of 3AP. Different experiments were conducted to analyse the effect of different operating parameters such as SBAC bed height, inlet concentration of 3AP solution and inlet flow rate of 3AP solution. All the experiments were performed by keeping constant pH of inlet stream at 6.5 and at room temperature.

The break-through time and exhaustion time were analysed at different operating conditions. The time required by effluent concentration to reach 10% of initial concentration was finalized as breakthrough time (t_b). The exhaustion time (t_{exh}) was the time of operation when effluent concentration reaches to the 90% of the 3AP inlet concentration. Breakthrough time and exhaustion time were determined when $\frac{C_t}{C_i} = 0.1$ and $\frac{C_t}{C_i} = 0.9$ (Faki et al., 2008) respectively. Total quantity of 3AP adsorbed q_{ads}(mg) in the fixed bed was estimated using following equation (Singh et al., 2016b):

$$q_{ads} = \frac{Q}{1000} \int_{t=0}^{t=t_{total}} C_{ads} dt \tag{3}$$

where t_{total} is total time for the operation (min), C_{ads} represents the 3AP adsorbed on SBAC and Q is the flow rate of 3AP solution (mL/min)

Maximum adsorption capacity, q_m (mg/g) was calculated using following equation (Sadaf et al., 2015):

$$q_m = \frac{q_{ads}}{m} \tag{4}$$

where q_{ads} (mg) is 3AP adsorbed and m is mass of SBAC (g) in the column.

2.5. Analysis

2.5.1. SBAC characterization

Brunauer–Emmett–Teller (BET) analysis was performed to analyse the available surface area for adsorption along with the pore volume/diameter data. Barrett–Joyner–Halenda (BJH) analysis was also performed to calculate adsorption/desorption pore volume and pore diameter. SEM images of adsorbent before and after use in the treatment were obtained using the SEM equipment (JEOL, USA).

2.5.2. Pollutant analysis

The analysis of concentration of pollutant (3AP) in the solution was carried out by UV analyser (model UV 1800, Shimazu). The wavelength of maximum absorption of 3AP was established by scanning the known concentration of 3AP solutions at different wavelength. The λ_{max} was recorded as 232 nm. A simple method based on UV was used in the current work for analysis as it was expected that reliable measurements can be obtained using UV spectrophotmetric analysis. As adsorption is physical removal of pollutant from solution, it is expected that there will not be any intermediates formed unlike oxidation reaction and hence no interference in the measurements is expected. Indeed, when the analysis was repeated at least two times to see the reproducibility of the experiments, the observed differences were typically within $\pm$1% of the reported average values for the analysis.

Calibration curve of 3AP was initially plotted by recording the absorbance of different solutions with known concentrations. The linearity coefficient (R^2) value was 0.999 confirming very good fitting. The values of the limit of detection (LOD) and limit of quantification (LOQ), obtained using the standard deviation and slope, were 0.27 and 0.83 mg/L respectively.

3. Results and discussion

3.1. SBAC characterization

The values of different parameters such as pore volume, diameter and surface area were obtained using the BET analysis. The observed surface area was 119.77 m^2/g. The BJH single point pore volume was observed to be 0.0920 cm^3/g whereas BJH adsorption/desorption pore volume was 0.02041/0.03164 cm^3. The average BET pore diameter was observed to be 18.624 Å while the BJH adsorption/desorption pore diameter was 24.624 A^0/64.12 A^0 which is considered good for the use in adsorption as per the presented comparison with literature. Lataye et al. (2011) reported that the BET surface area of rice husk ash (RHA) used for treatment of 4-picoline was 65.36 m^2/g whereas the BJH cumulative pore volume for single point was 0.057 cm^3/g. Daware et al. (2014) reported that the BET surface area for agro coal ash applied for removal of 2-picoline from wastewater was 58.2 m^2/g. Hashemian and Mirshamsi (2012) reported 65 m^2/g as the BET surface area for saw dust used for removal of 2-picoline. In the same study, the average pore diameter and total pore volume were reported to be 35 A^0 and 0.0056 cm^3/g respectively. The BET analysis gives idea about pore size and surface area with typical guideline of, higher the BET surface area, higher will be the adsorption capacity. In the present study, obtained results for the BET and BJH analysis displayed better efficiency in comparison with literature reporting the other adsorbents confirming the usefulness of SBAC. It is also important to note that the present work was based on acid activation during the synthesis which also helps in imparting functionality to adsorbent enhancing the interactions of the pollutant molecules with the adsorbent yielding better removal efficacy.

The obtained SEM images for the native adsorbent before use in the adsorption shows several level of cavities, porosity and, irregular adsorbent surface (Fig. S2(a) provided in supplementary data). SEM Images after adsorption (Fig. S2(b) provided in supplementary data) clearly depicts the loading of 3AP based on filled in cavities on the surface or inside the pores. The analysis allowed establishing the governing mechanisms for the adsorption of the pollutant molecules inside the pores and on the surface of the adsorbent.

3.2. Batch adsorption studies

3.2.1. Effect of pH on the removal of 3AP

The adsorption of 3AP is strongly affected by pH as the form of compound is affected by the value of pH based on the dissociation constant and hence it is essential to understand the effect of pH on the extent of adsorption in greater details for specific system. The obtained pH effect on 3AP removal, at initial concentration of 100 mg/L and temperature of 303 K, has been shown in Fig. 1(a) and (b). It has been observed that extent of removal of 3AP increases with a change in pH from 2 to 7.5, though only marginal change is observed between the ranges of 6.5 to 7.5. Quantitatively, 3AP removal at

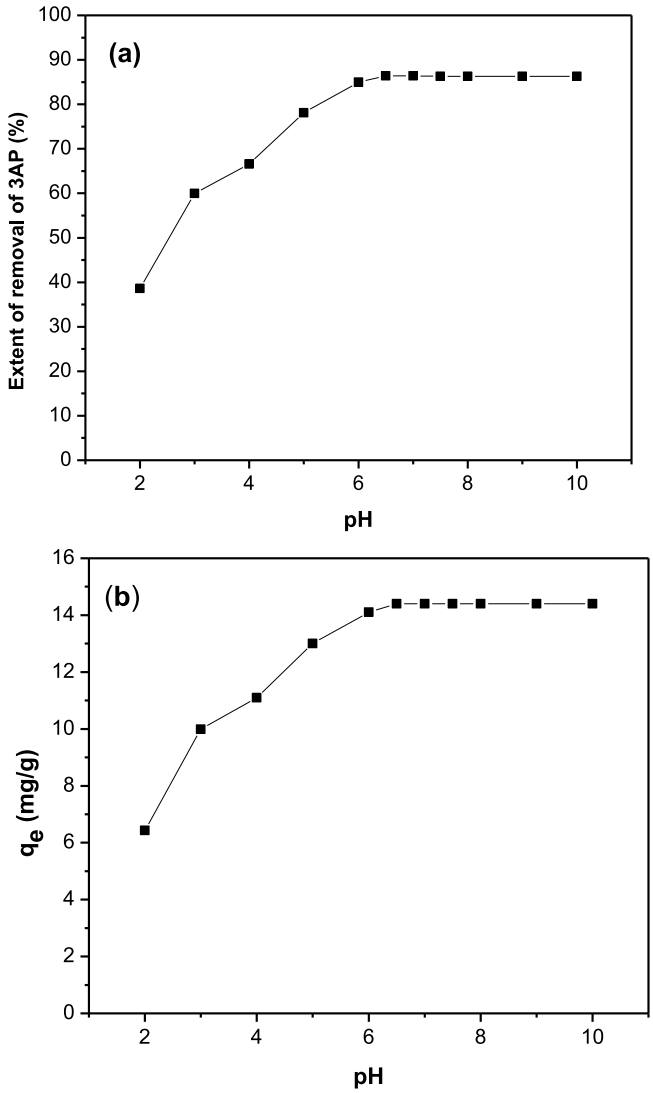

Fig. 1. Effect of pH on the removal of 3AP using SBAC adsorbent (T = 303 K, t = 300 min, C_i = 100 mg/L, w = 6 g/L): (a) Extent of removal; (b) amount of 3AP adsorbed.

pH equal 2 was around 34%, which increased to 86.5% with an increase in the pH to 6.5 and further increase of pH to 7.5 changed the extent of removal to 86.7%. 3AP has pKa value of 6.4 which indicates that adsorbate has a favourable state at pH higher than 6.4 favouring adsorption and lower interactions are expected at pH lower than 6.4. The chemical interaction of 3AP with SBAC can be written as follows

$3AP + H^+ \longrightarrow 3APH^+$

$3AP + SBAC \longrightarrow 3AP - SBAC$

$3APH^+ + M^+ - SBAC \longrightarrow 3APH^+ - SBAC + M^+$

$H^+ + 3APH^+ - SBAC \longrightarrow H^+ - SBAC + 3APH^+$

$H^+ + SBAC \longrightarrow H^+ - SBAC$

$3AP - H^+ - SBAC \longrightarrow 3APH^+ - SBAC$

Bagasse activated carbon generally contains metal oxides on its surface (Lataye et al., 2006). M^+ represents exchangeable cation on the adsorbent surface (Mohan et al., 2004). It is also important to understand that 3AP has two adsorption sites, one at hetero N atom and second at amino group. At low pH, lone pair electrons on two nitrogen atoms are not free and hence adsorption is found to be the minimum. At lower pH, the 3AP is likely to be converted to 3 APH^+ due to protonation which results in a decrease in adsorption of 3AP (Alam and Kamaluddin, 2000b) The extent of protonation reduces with an increase in the pH and hence higher extents of removal are obtained. Thus, at high values of pH (pKa, 6.4 $<$ pH), adsorption of 3AP was found to be increase on positively charged surface of adsorbent because of the presence of

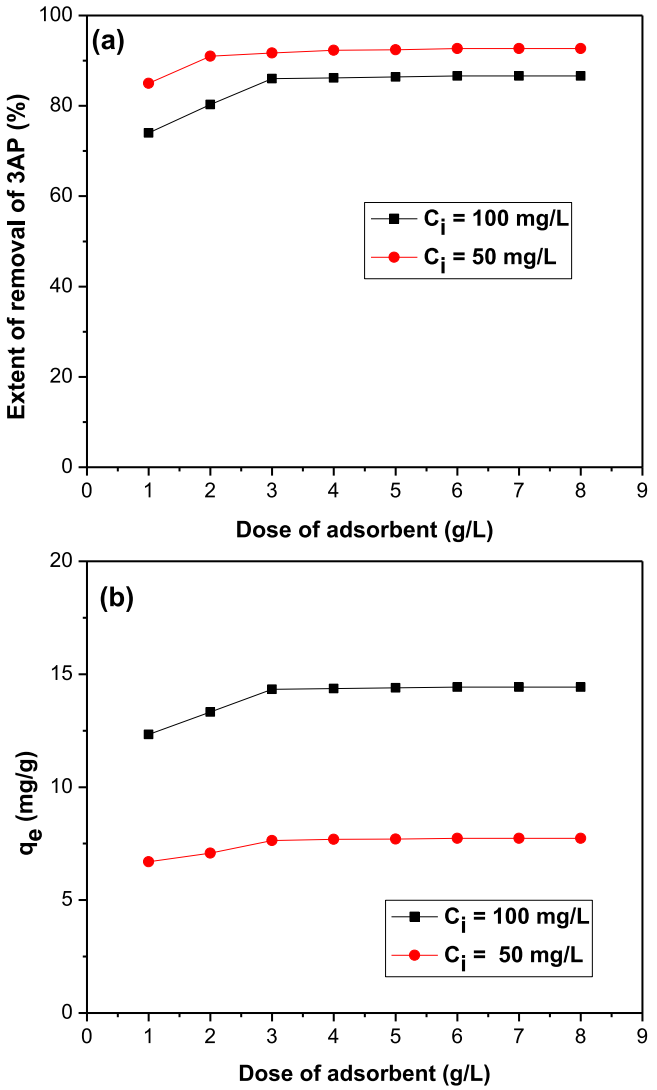

Fig. 2. Effect of adsorbent dose on the removal of 3AP using SBAC adsorbent (T = 303 K, t = 300 min, pH 6.5): (a) Extent of removal at two different concentrations as C_i = 50 mg/L and C_i = 100 mg/L; (b) amount of 3AP adsorbed (q_e) at C_i = 50 mg/L and C_i = 100 mg/L.

unprotonated 3AP molecules in the solution. Further increase in the pH beyond pH of 6.5 does not contribute favorably and hence there is not much change in extent of removal. The dominant adsorption mechanism is thus the direct interaction of the pollutant molecule with adsorbent whereas the adsorption in the protonated forms of 3AP contributes only marginally. Similar observations for the effect of pH were reported for the removal of 2-methylpyridine using bagasse fly ash (Lataye et al., 2008). Xia et al. (2018) also reported that the maximum removal of pyridine was obtained at pH 7. Singh et al. (2016a) reported similar trends for adsorption of pyridine on mesoporous silica. Considering the obtained results in the work, further adsorption studies were performed at pH 6.5.

3.2.2. Effect of SBAC dose on the removal of 3AP

The obtained results for effect of SBAC dose on the extent of removal and amount of 3AP adsorbed are represented in Figs. 2(a) and 2(b) respectively under conditions of initial concentrations of 50 mg/L and 100 mg/L and pH of 6.5. It can be seen from Fig. 2(a) at 2 g/L as the adsorbent dose, extent of 3AP removal was found to be 69% for the case of initial concentration of 100 mg/L. The extent of removal increased dominantly from 69% to 84.4% with an increase in SBAC dose from 2 to 4 g/L but a further increase in the SBAC dose from 4 to 6 g/L resulted in a marginal change in the extent of removal from 84.4 to 86.3% at fixed concentration as 100 mg/L. It can be thus said that 6 g/L dose is the optimum and beyond this optimum, the extent of removal is marginally affected due to possible aggregation of sites available for adsorption due to significant adsorbent particle–particle interaction. Similar trends were also reported by Jain and Gogate

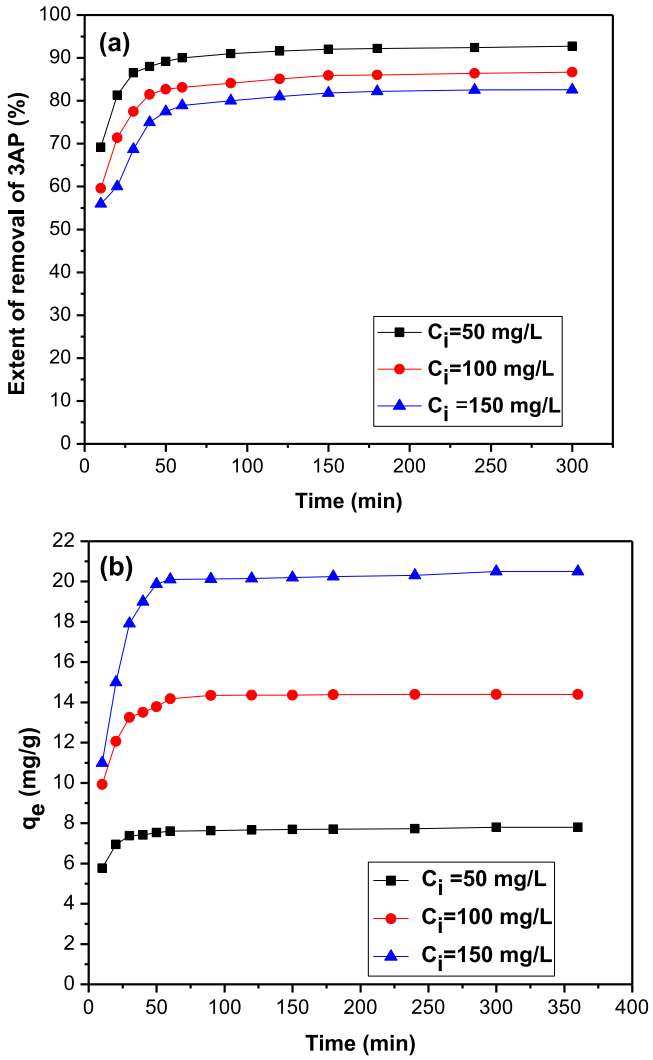

Fig. 3. Effect of contact time on the removal of 3AP using SBAC (T = 303 K, t = 300 min, w = 6g/L, pH = 6.5): (a) Extent of removal (b) amount of 3AP adsorbed (q_e)

(2017a) with the extent of removal for H_2SO_4 activated bioadsorbent increasing from 43.3% to 86.4% with an increase in bioadsorbent loading from 1 to 5 g/L. Subsequently increasing the loading from 5 g/L to 10 g/L resulted in only a marginal change in the extent of removal attributed to the aggregation of sites. Lataye et al. (2008) investigated adsorption of 2-picoline on bagasse fly ash (BFA) where the optimized adsorbent dose was reported as 5 g/L with very less increment in extent of removal observed beyond 5 g/L. Comparison with literature allowed establishing that though the trends are similar, the exact value of optimum loading is different for each adsorbent and hence there is a need for the detailed study as demonstrated in the current work.

It can be also seen from Fig. 2(a) and (b), though similar trends were observed for the case of 50 mg/L as the initial concentration, the extent of removal of 3AP was higher at initial concentration of 50 mg/L (92.1%) compared to 100 mg/L (86.3%). It is important to note that equilibrium amount of 3AP adsorbed at initial concentrations of 100 mg/L and 50 mg/L are 14.43 mg/g and 7.73 mg/g respectively. The obtained trends confirmed that the active sites on the adsorbent are better utilized due to the higher concentrations of the pollutant before the equilibrium is reached.

3.2.3. Effect of contact time on extent of removal

The effect of contact time on the extent of 3AP removal at different initial concentrations has been shown in Fig. 3(a). It was observed that the adsorption was very fast during initial stage and within 30 min almost 70%–80% removal was obtained at all the initial concentrations investigated in the study. Maximum extent of removal was obtained in 180 min of treatment time and beyond this treatment time, only marginal change was obtained in the extent of removal of 3AP

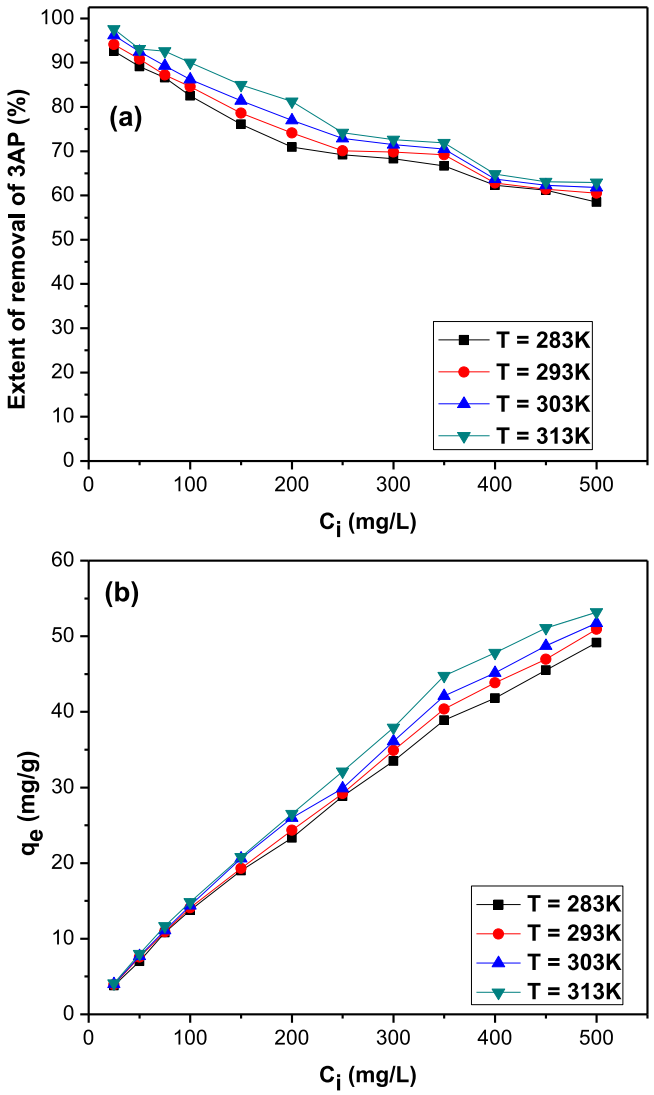

Fig. 4. Effect of initial concentrations on the removal of 3AP using SBAC (t = 300 min, pH 6.5, w = 6 g/L): (a) Extent of removal (b) amount of 3AP adsorbed (q_e)

till treatment time of 300 min. The extent of removal of 3AP remained unchanged beyond 300 min (data beyond 300 min not shown for clarity in figures) and hence all the experiments were conducted at constant batch time as 300 min.

The rate of adsorption at the beginning is very high as more active sites are available for adsorption and during later stages, the adsorption rate was found to decrease significantly due to the fact that the adsorbent surface gets exhausted and equilibrium is also reached between the adsorbed 3AP and the residual quantum in the solution. Hashemian and Parsaei (2015) reported similar observation for adsorption of 2-picoline and 3-amino-2-picoline on Kaoline. Fast adsorption was observed during initial stages with adsorption of pollutant increasing rapidly till 80 min, and beyond 80 min, the extent of removal was found to be unchanged as the surface of adsorbent got exhausted. Similar observation was reported by Daware et al. (2014) for 2-picoline adsorption on agro coal ash with very fast adsorption during first hour and reducing rate of adsorption in later stages as the adsorbent surface got saturated. The maximum extent of removal was noticed till 7h, beyond which no increase in adsorption was reported. It is again imperative to understand that the time required for reaching the equilibrium is indeed different for each case and hence the detailed study reported in the current work is very relevant.

3.2.4. Effect of initial 3AP concentration

Experiments were performed over a broad span of 3AP initial concentrations as 25–500 mg/L keeping SBAC dose constant at 6 mg/L, batch time at 300 min and maintaining pH of 6.5. The obtained results are demonstrated in Fig. 4(a)

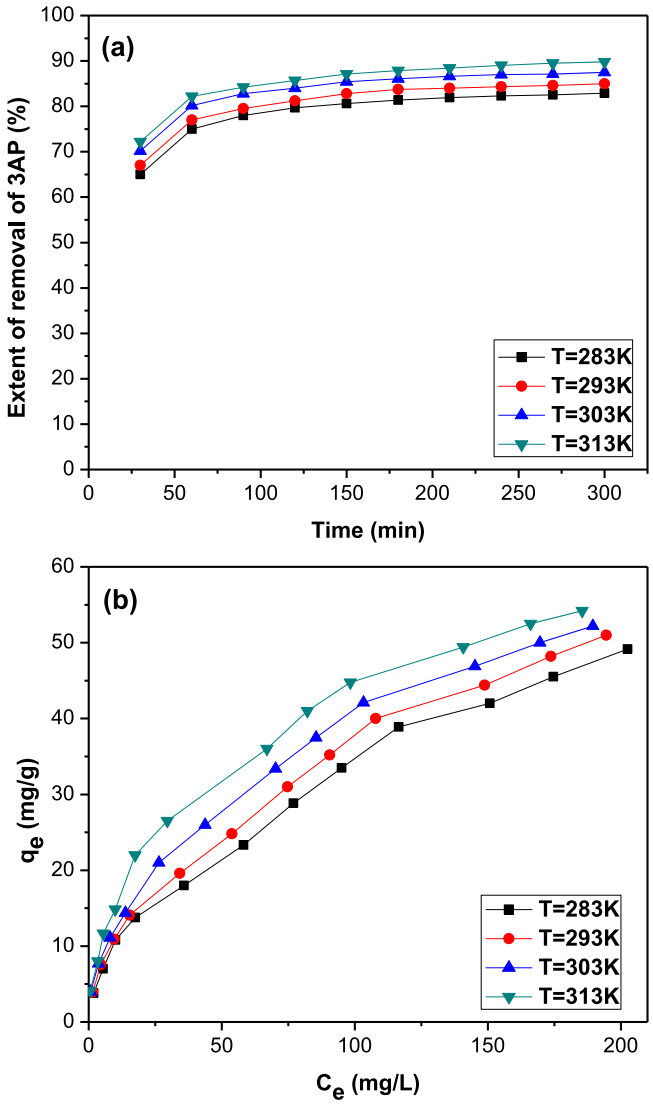

Fig. 5. Effect of Temperature on (a) Extent of removal of 3AP (C_i = 100 mg/L, t = 300 min, pH = 6.5, w = 6 g/L). (b) Equilibrium adsorption capacity of SBAC at different equilibrium concentrations (t = 300 min, pH = 6.5, w = 6 g/L).

in terms of extent of removal. It can be seen from the figure that the maximum extent of removal was observed to be 97.6% at 25 mg/L and 62.1% at 500 mg/L as the initial concentration. It was observed that the extent of removal of 3AP decreases with an increase in initial concentration, which can be attributed to the fact that a fixed quantity of adsorbent is available which is not efficient in removing excess molecules of 3AP present in the solution. At higher concentration of 3AP, the adsorbent gets saturated earlier and some of the molecules of 3AP remain unabsorbed in the solution.

The obtained results for the actual adsorption capacity have been shown in Fig. 4(b). It was observed as concentration increases, the loading of 3AP on SBAC increases even though the percentage removal reduced. Quantitatively, the amount of 3AP adsorbed on SBAC at 500 mg/L as initial concentration was found to be 54.4 mg/g and only around 5 mg/g at 25 mg/L as the initial concentration of 3AP. The enhanced amount of 3AP adsorbed on SBAC with an increase in the initial concentration of 3AP is attributed to the enhanced mass transfer giving more interaction of 3AP with the adsorbent in the solution. Jain and Gogate (2017b) also reported similar trends for treatment of acid blue 25 dye on biosorbent. The amount of dye adsorbed increased from 12.4 mg/g to 47.25 mg/g by increasing dye concentration from 50 mg/L to 200 mg/L. As a good representation of the initial concentration and based on trade off between extent of removal and adsorbent utilization in terms of adsorption capacity, initial concentration of 100 mg/L has been chosed for further studies in the current work.

3.2.5. Temperature effect on removal of 3AP

Experiments were performed over temperature range of 283 K to 313 K at fixed initial concentration of 100 mg/L and the obtained results have been depicted in Fig. 5(a) and (b). It can be clearly seen from Fig. 5(a) that the extent of removal 3AP increases from 82.5% to 89.6% with an increase in temperature from 283 K to 313 K. Fig. 5(b) depicts the temperature effect on the variation in the equilibrium adsorption capacity of SBAC with equilibrium concentration. It can be seen from Fig. 5(b) that the amount of 3AP adsorbed was 45.9 mg/g at 283 K, which increased to maximum of 54.4 mg/g at 313 K with a marginally lower value of 52.1 mg/g at 303 K. Overall an increase in the removal of 3AP is obtained with an increase in the temperature of the solution. Increase in temperature enhances the vibrations of molecules which increases the mobility of molecules (Mohan et al., 2005) and hence the diffusivity leading to deeper penetration of 3AP inside the adsorbent. It was also observed that the increase in the adsorption capacity was marginal beyond temperature of 303 K and hence all the subsequent experiments were conducted at 303 K. Temperature of 303 K also corresponds to the ambient temperature and hence minimum energy requirement is expected for maintaining the temperature.

Lataye et al. (2011) reported similar trends for the 4-Methylpyridine adsorption on BFA and rice husk ash (RHA). It was reported that adsorption capacity increased from 50 mg/g to 60 mg/g and 15 mg/g to 19 mg/g on BFA and RHA respectively by increasing temperature from 283 K to 313 K. Hashemian and Mirshamsi (2012) also reported that as temperature increases from 283 K to 323 K, the amount of 2-picoline adsorbed on saw dust for 60 mg/L as the initial concentration was found to increase from 425 mg/g to about 450 mg/g. Thus it is important to understand that though the trends are similar, the extent of increase in the adsorption capacity is different and so are the optimum temperatures establishing the importance of the study.

3.2.6. Kinetic study of 3AP adsorption

3.2.6.1. Pseudo first-order kinetic model. The mathematical form of the pseudo first–order kinetics model is represented by following equation (Weber and Morris, 1963):

$$\log(q_e - q_t) = \frac{-k_f t}{2.303} + \log q_e \tag{5}$$

where, q_e is the maximum amount of 3AP adsorbed on SBAC (mg/g) at equilibrium and k_f is rate constant in min^{-1}, q_t (mg/g)is the amount of 3AP adsorbed on SBAC at time 't' in min. The obtained values of q_e and k_f using the curve fitting for Eq. (5) (Fig. 6(a)) have been illustrated in Table 1. However, it can be observed the R^2 values are not near to unity which indicates the experimental data is not giving best fitting to pseudo first-order kinetics.

3.2.6.2. Pseudo second-order model. The pseudo second order model of adsorption is represented by following equation (Blanchard et al., 1984):

$$\frac{t}{q_t} = \frac{t}{q_e} + \frac{1}{q_e^2 k_s} \tag{6}$$

where k_s is rate constant (g mg^{-1} min^{-1}).

The obtained values of the rate constants using the curve fitting for Eq. (6) (Fig. 6(b), experimental data at equilibrium and R^2 are represented in Table 1. It can be seen that the values of R^2 are close to one. The values of both calculated and experimental q_e are also close to each other. The obtained data confirmed the best fitting of pseudo second order kinetic model for the present work. Similar trend has also been reported for pyridine removal using agro based bio-composite (Bageru and Srivatav, 2018). Gautam et al. (2013) also reported that pseudo second order model fitted best for removal of Alizarin Red S using mustard husk.

3.2.6.3. Elovich model. The model is based on the governing mechanism of adsorption as chemisorption and the mathematical form of Elovich model is depicted by following equation (Jia et al., 2017)

$$q_t = \frac{1}{\beta}\ln(\alpha\beta) + \frac{1}{\beta}\ln(t) \tag{7}$$

where, β is a constant related to the extent of covered surface, and α is a constant deciding the contribution of chemisorption (Belaid et al., 2013). The graph of $\ln t$ versus q_t (Fig. 6(c)) was plotted to quantify the values of α and β. Elovich equation, initially used to express the beginning of sorption process, long time before equilibrium, can be used correctly in the case of chemisorption with heterogeneous materials. The obtained values of α, β and R^2 are summarized in Table 1. It has been observed the R^2 values are significantly deviating from unity in comparison with pseudo second order model which indicates the Elovich model was not suitable, also confirming that the chemisorption is not the controlling adsorption mechanism. Similar trends were reported by Makrigianni et al. (2015) for adsorption of phenol over pyrolytic tyre char.

3.2.7. Fitting of adsorption isotherms

Different isotherms such as Freundlich, Langmuir and Temkin were used to correlate the data obtained at the equilibrium experimentally as represented in Table 2. We now present the basic governing equations for the different isotherms.

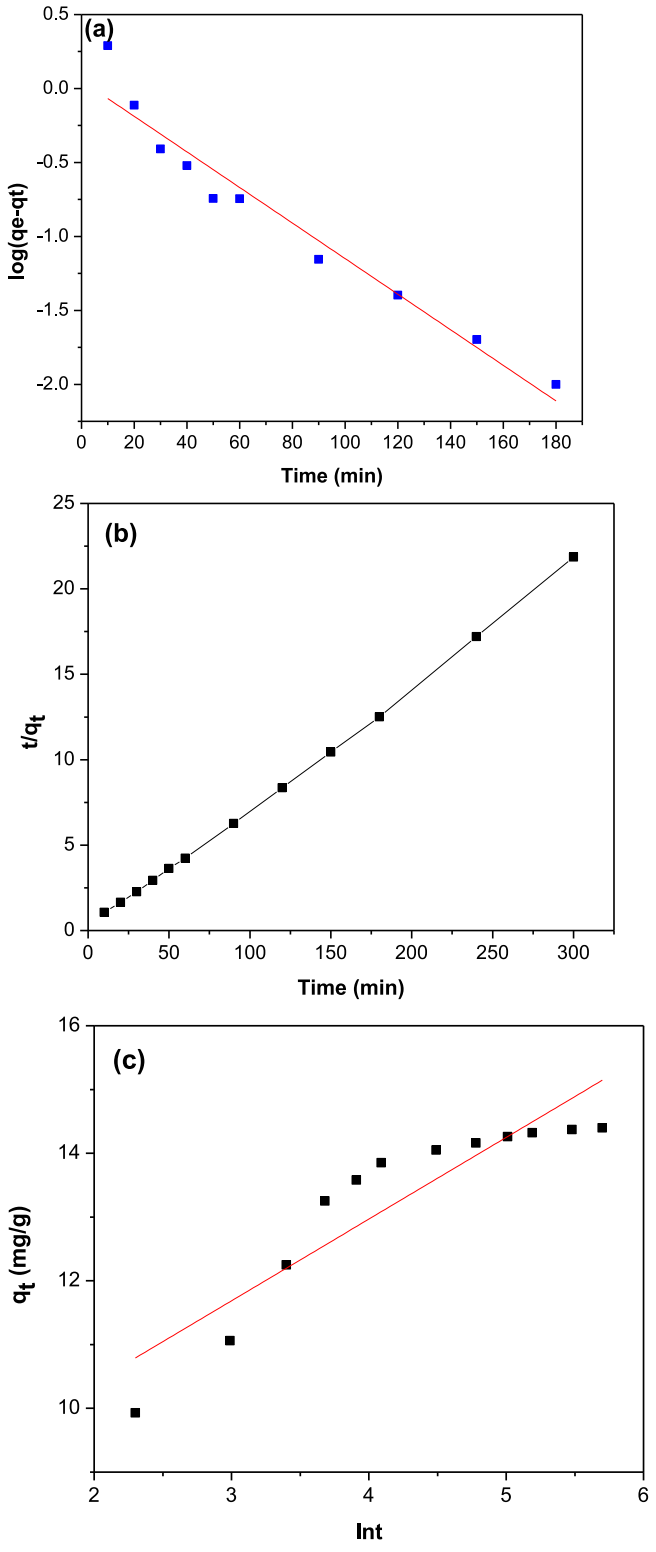

Fig. 6. Kinetics model fitting for batch data obtained for removal of 3AP under condition of C_i = 100 mg/L, T = 283 K, pH = 6.5 and w = 6 g/L for (a) Pseudo-First order model, (b) Pseudo-Second order model, (c) Elovich model.

Table 1
Kinetic parameters for removal of 3 AP using SBAC (T = 303 k, t = 300 min, pH = 6.5, w = 6 g/L).

Pseudo-first order	c_i (mg/L)	50	100	150
	q_{exp} (mg/g)	7.75	14.36	20.85
	q_e (mg/g)	1.127	3.6	10.42
	k_f (min^{-1})	0.0276	0.0368	0.04836
	R^2	0.95	0.884	0.945
Pseudo-second order	c_i (mg/L)	50	100	150
	q_{exp} (mg/g)	7.75	14.36	20.85
	q_e (mg/g)	7.80	14.38	20.83
	k_f (min^{-1})	0.06455	0.0359	0.01023
	h (mg $g^{-1}min^{-1}$)	3.92	7.42	4.43
	R^2	1	0.9983	0.9988
Elovich model	c_i (mg/L)	50	100	150
	α (mg $g^{-1}min^{-1}$)	115.6	564	1930
	β (g mg^{-1})	2.534	1.289	1.055
	R^2	0.683	0.882	0.84

Table 2
Isotherm parameters for adsorption of 3AP on SBAC (t = 300 min, pH = 6.5, w = 6 g/L).

Isotherm model	parameters	Values			
Langmuir	T (K)	283	293	303	313
	k_L (L/mg)	0.023	0.027	0.028	0.041
	q_m (mg/g)	53.47	53.76	54.66	54.94
	R^2	0.9888	0.989	0.9936	0.995
	MPSD	0.266	0.315	0.338	0.484
	ARE	1.131	1.2237	1.287	1.338
Freundlich	k_F (L/mg)	3.098	3.6	3.97	5.13
	1/n	0.5289	0.5083	0.5056	0.455
	R^2	0.984	0.9831	0.985	0.983
	MPSD	0.0901	0.1159	0.1546	0.180
	ARE	0.805	0.914	0.939	0.942
Temkin	B1	9.887	9.823	9.91	9.016
	k_T	0.399	0.4838	0.514	0.858
	R^2	0.944	0.9557	0.9558	0.9479
	MPSD	3.47	2.36	2.56	5.10
	ARE	3.04	2.92	2.93	3.39

3.2.7.1. Freundlich and Langmuir isotherm models. Freundlich isotherm is typically applicable to adsorption process that occurs on heterogeneous surfaces. This isotherm gives an expression which defines the surface heterogeneity and the exponential distribution of active sites and their energies. The linearized form of adsorption model for Freundlich Isotherm is represented by Eq. (8) (Freundlich, 1906)

$$\ln q_e = \ln k_F + \frac{1}{n} \ln c_e \tag{8}$$

where q_e(mg/g) is the uptake capacity of SBAC at equilibrium, c_e is equilibrium concentration, k_F is the measure of adsorbent capacity and $\frac{1}{n}$ is the model parameter.

Langmuir isotherm is found to be true for monolayer adsorption on adsorbent. Mathematically, the isotherm is represented using following equation (Langmuir, 1947)

$$\frac{c_e}{q_e} = \frac{1}{k_A q_m} + \frac{c_e}{\mathrm{q_m}} \tag{9}$$

where, q_m is maximum monolayer adsorption capacity in mg/g as per Langmuir model and k_A is the constant for the Langmuir model.

3.2.7.2. Temkin isotherm model. Eq. (10) represents the mathematical form of the Temkin Isotherm (Temkin and Pyzhev, 1940)

$$q_e = \frac{RT}{b} \ln(k_T c_e) \tag{10}$$

The linear form of Eq. (10) can be represented by following equation.

$$q_e = B_1 \ln k_T + B_1 \ln c_e \tag{11}$$

where, $B_1 = \frac{RT}{b}$ is Temkin energy constant, k_T is the model constant representing interaction between 3AP and SBAC and q_e is adsorption capacity of SBAC at equilibrium.

To find best fitting for the models, graphs were plotted for Freundlich ($\ln q_e$ *vs* $\ln c_e$), Langmuir ($\frac{C_e}{q_e}$ *vs* c_e) and Temkin (q_e vs $\ln c_e$) isotherms as shown in Fig. 7(a)–(c). The obtained values of R^2 for Freundlich isotherm as shown in Table 4 confirm that the R^2 values are in proximity of unity (around 0.99). Similarly for the Langmuir isotherm, the R^2 values are in proximity of unity (around 0.989). For Temkin model, values of R^2 were nearer to 0.94.

3.2.7.3. Error analysis. To examine the suitableness of the isotherm model, different approaches of error analysis have also been employed.

Marquardt's percent standard déviation (MPSD) **:**

MPSD [Marquardt (1963)] is widely used to examine the suitability and correctness of the model fitting with the experimental data. The error function is represented by following equation

$$\text{MPSD} = 100 \sqrt{\frac{1}{n-p} \sum_{i=1}^{n} \left(\frac{(q_{e,\text{exp}} - q_{e,\text{calc}})}{q_{e,\text{exp}}} \right)_i^2} \tag{12}$$

The MPSD error function has been often used by many researchers (Mane et al., 2007). Here, $q_{e,\text{calc}}$ and $q_{e,\text{exp}}$ are the calculated and the experimental values of equilibrium adsorption capacities (mg/g) respectively, n is the number of data points and p is the number of parameters in the isotherm equation.

Average Relative Error (ARE):

The average relative error **(**ARE) (Kapoor and Yang, 1989) values are calculated using following equation

$$\text{ARE} = \frac{100}{n} \sum_{i=1}^{n} \left| \frac{(q_{e,\text{exp}} - q_{e,\text{calc}})}{q_{e,\text{exp}}} \right|_i \tag{13}$$

where, n is the number of data points.

The values obtained for MPSD and ARE were observed to be minimum (Table 2) for Freundlich and Langmuir compared to the Temkin model. The obtained R^2 values for Freundlich and Langmuir were also close to unity and it can be thus said that Langmuir and Freundlich are best suited for explaining the adsorption of 3AP on SBAC as compared to the Temkin model. Similar trend has also been reported for pyridine removal using activated carbon (Mohan et al., 2004).

3.2.8. Thermodynamic study

Van't Hoff equation is represented by Eq. (14), which is important thermodynamic equation normally used to check the feasibility/spontaneity of the operation and predict the heat of adsorption (Jain et al., 2010).

$$\Delta G^0 = -RT \ln K \tag{14}$$

Gibb's free energy can be estimated based on following equation:

$$\Delta G^0 = \Delta H^0 - T\Delta S^0 \tag{15}$$

ΔG^0 values determine the adsorption feasibility whereas the ΔS^0 values determine spontaneity of adsorption. Combining Eqs. (14) and (15) gives,

$$\ln K = \frac{-\Delta G^0}{RT} = \frac{\Delta S^0}{R} - \frac{\Delta H^0}{R} \frac{1}{T} \tag{16}$$

The value of ΔH^0 and ΔS^0 were determined by plotting the graph for *lnK* versus $\frac{1}{T}$ represented in Fig. S3 (supplementary data). The obtained negative ΔG^0 values (Table 3) confirmed that adsorption is feasible. The increase in negative value of ΔG^0 with an increase in temperature from 283 K to 313 K also confirmed favourable adsorption conditions. The positive ΔS^0 (Table 3) values confirmed the affinity of 3AP towards SBAC and spontaneity of adsorption.

For all the three isotherms studies, ΔH^0 was obtained as > 0. For example Langmuir fitting resulted in value of 11.71 kJ/mol whereas for Freundlich, it was observed to 10.23 kJ/mol and for Temkin, the value of $\Delta H^0$was 15.43 kJ/mol. The obtained values indeed confirmed endothermic nature of adsorption. Same kind of observation has been reported for treatment of most of pyridine derivatives (Daware et al., 2014; Lataye et al., 2011). In the present work, the obtained values of ΔH^0 ($<$40 kJ/mol) indicated 3AP adsorption over SBAC is physical in nature (Ozturk and Kavak, 2005).

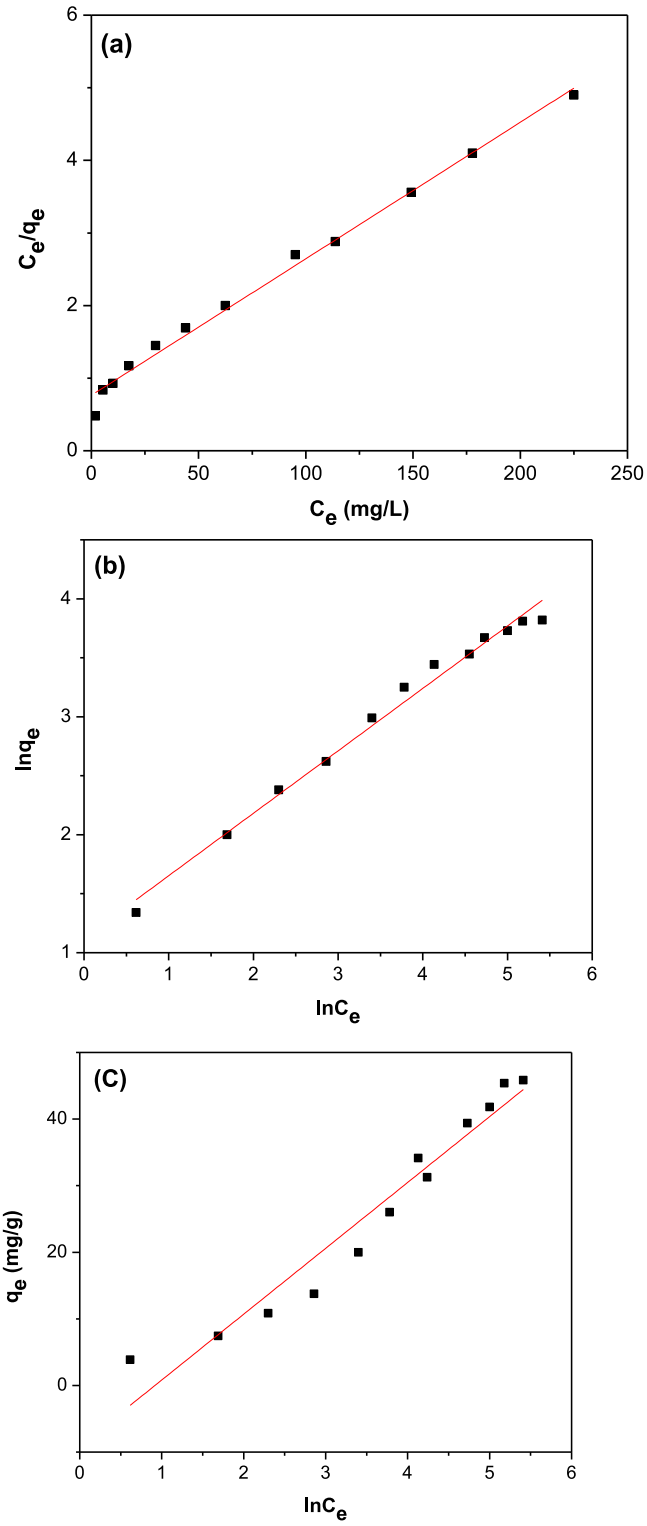

Fig. 7. Adsorption isotherm plots for adsorption of 3AP on SBAC under condition (T = 293 K, pH = 6.5, w = 6 g/L. (a) Langmuir (b) Freundlich (c) Temkin.

Table 3
Thermodynamic parameters for adsorption of 3AP on SBAC at different Temperatures.

Isotherm model	ΔG^0 (kJ/mol)				ΔH^0	ΔS^0
	283 K	293 K	303 K	313 K	(kJ/mol)	(kJ/mol K)
Langmuir	−18.06	−19.09	−19.82	−21.84	11.71	0.1047
Freundlich	−29.60	−31.25	−32.32	−34.05	10.23	0.0829
Temkin	−24.60	−26.12	−27.17	−29.40	15.43	0.141

Table 4
Details of breakthrough and exhaust time at different bed height (H), initial concentration (Ci) and flow rate (F).

H (cm)	Q (mL/min)	c c_i (mg/L)	t_b (min)	t_e (min)	q_{exp} (mg/gm)
3	8	100	50	140	49.86
4	8	100	80	180	53.19
5	8	100	115	240	65.6
3	6	100	80	170	54.14
3	9	100	30	110	42.97
3	8	50	75	170	36.75
3	8	150	30	100	56.03

3.2.9. Regeneration study

In order to check feasibility of adsorbent for subsequent reuse, regeneration study is important. The regeneration of SBAC has been studied using different eluents as 0.1N H_2SO_4, 01N NaOH, distilled water and ethanol. For the regeneration study, the used adsorbent (3AP loaded on SBAC) was mixed with 50 mL of eluent (overall solid loading of 150 mg/L), kept in orbital shaking incubator and allowed to interact for 300 min at 303 K. The desorption efficiency was estimated using following equation (Seki and Yurdakoc, 2006).

$$\text{Extent of desorption}(\%) = \frac{C_{des}}{C_{ads}} \times 100 \tag{17}$$

The maximum regeneration of 3AP was observed in ethanol. The extent of desorption of 3AP was 54.1% in 0.1N H_2SO_4, 30% in 0.1N NaoH, 10.52% in water and maximum of 74.9% in ethanol (as shown in Fig. 8(a)). The regeneration was observed to be high in acidic condition (0.1N H_2SO_4 medium as compared to base (0.1N NaOH) which is due to the fact that 3AP is weak base and hence acidic medium favours desorption of 3AP. The extent of desorption was observed to be maximum in ethanol due to the very high solubility of 3AP in ethanol which increases the affinity of 3AP towards ethanol. The recovered SBAC were further used for 3AP adsorption. Reuse experiments were conducted for five cycles of regeneration followed by adsorption. The extent of desorption was found to decrease from 74.9% after first cycle to 68.49% after 5 cycles. The adsorption capacity in the actual adsorption experiments also decreased from 21.9 mg/g in the first cycle to 15.01 mg/g in fifth cycle as shown in Fig. 8b. The reduction in the adsorption capacity during the reuse is attributed to the fact that residual 3AP is present on the active sites of the SBAC as 100% desorption is not achieved. After one cycle, 25.1% of 3AP still remains on the active sites (as only 74.9% desorption takes place) of SBAC and hence the available active sites decreases for second cycle. As cycles of adsorption–desorption continues, the adsorption capacity decreases as more active sites are blocked by the 3AP. Overall, the decrease in the adsorption capacity can be attributed to the loss in active sites of SBAC based on permanent adsorption of 3AP. Though there is not much effectiveness for reusability, it can be said that the SBAC preparation cost is very less and hence after use in optimum number of cycles (to be established based on detailed study as highlighted in the current work), SBAC can be incinerated and this can also give some calorific value benefits. Off course proper scrubbing needs to be provided to take care of any exhaust gases.

Lataye et al. (2006) reported similar observations for poor regeneration of used adsorbent for adsorption of pyridine with the desorption efficiency of 68% in ethanol and 51% in 0.1N H_2SO_4. Xia et al. (2018) reported similar trends for system of pyridine adsorption using lignosulfonate intercalated layered double hydroxide (LS-LDH). It was reported that for regeneration using acetone as solvent, the desorption efficiency decreased from 84% in the first cycle to 55% after 10^{th} cycle.

3.3. Adsorption experiments in column operation

3.3.1. SBAC bed height effect

Adsorption of 3AP has been studied in the column operation at varying fixed bed height as 3, 4 and 5 cm at influent concentration of 100 mg/L and flow rate of 8 mL/min. The results in Table 4 and Fig. 9(a) shows that as the bed height increases, the time required for reaching the breakthrough point and exhaustion time increases which is attributed to increased quantity of adsorbent being available at higher bed height that ultimately enhances the surface area of SBAC and contact time. At lower SBAC bed height, 3AP molecules does not get enough contact time so as to utilize SBAC completely resulting in decreased SBAC capacity.

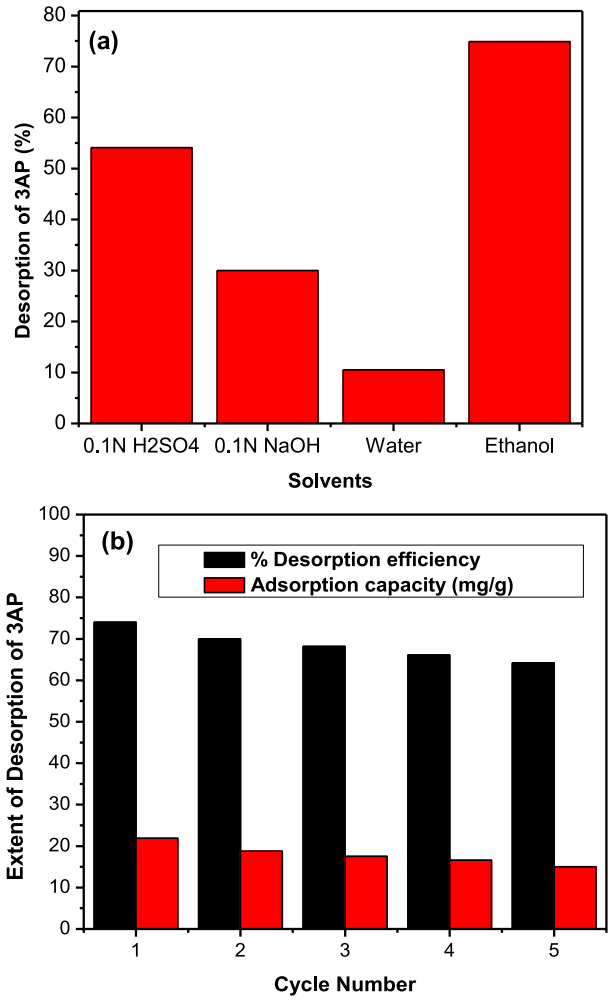

Fig. 8. (a) Dependency of desorption of 3AP on different solvents. (b) Regeneration efficacy and performance for adsorption in five cycles using Ethanol as eluent (*Y* axis also shows adsorption capacity with unit of mg/g as mentioned in legend).

As depicted in Table 4, it was seen that as the SBAC bed height increases from 3 cm to 5 cm, the breakthrough time increases from 50 min to 115 min and the exhaustion time increases from 140 min to 240 min. Also the amount of 3AP adsorbed increases from 49.86 mg/g to 65.6 mg/g. As the SBAC bed height increases, the slope of breakthrough curve decreases and the steeper curve was obtained at lower bed height. From these observations, it is clear that the performance of column in terms of removal enhances in the case of larger SBAC bed height.

Ramavandi et al. (2014) investigated the performance of orange dye adsorption at varying bed height from 3 cm to 7 cm and reported that as the bed height of adsorbent increases, the time for exhaust and breakthrough increases and also amount of dye adsorbed on adsorbent increases. Goel et al. (2005) illustrated similar observations for adsorption of lead, though quantitative values in terms of the extent of changes and the actual adsorption capacity were different.

3.3.2. Effect of 3AP initial concentration

Influence of various initial concentrations as 50, 100 and 150 mg/L on the breakthrough operation has been investigated at fixed bed height as 3 cm and constant 3AP solution inlet flow rate. It has been observed that as influent concentration increases, the breakthrough time and exhaustion time decreases whereas SBAC capacity increases, attributed to early bed saturation occurring at higher concentrations due to the fact that same quantity of SBAC is available in the column. The obtained parameter values are represented in Table 4 whereas the trends are represented in Fig. 9(b). Under conditions of 3 cm as SBAC bed height, 50 mg/L as inlet concentration and flow rate as 8mL/min, time for breakthrough was found to be 75 min and exhaustion time was 170 min. For the initial concentrations as 100 and 150 mg/L, breakthrough time decreased to 50 min and 30 min respectively. As influent concentration of 3AP increases, the observed rate of mass transfer also increases due to higher driving force and time required for complete loading of 3AP on adsorbent decreases. The overall

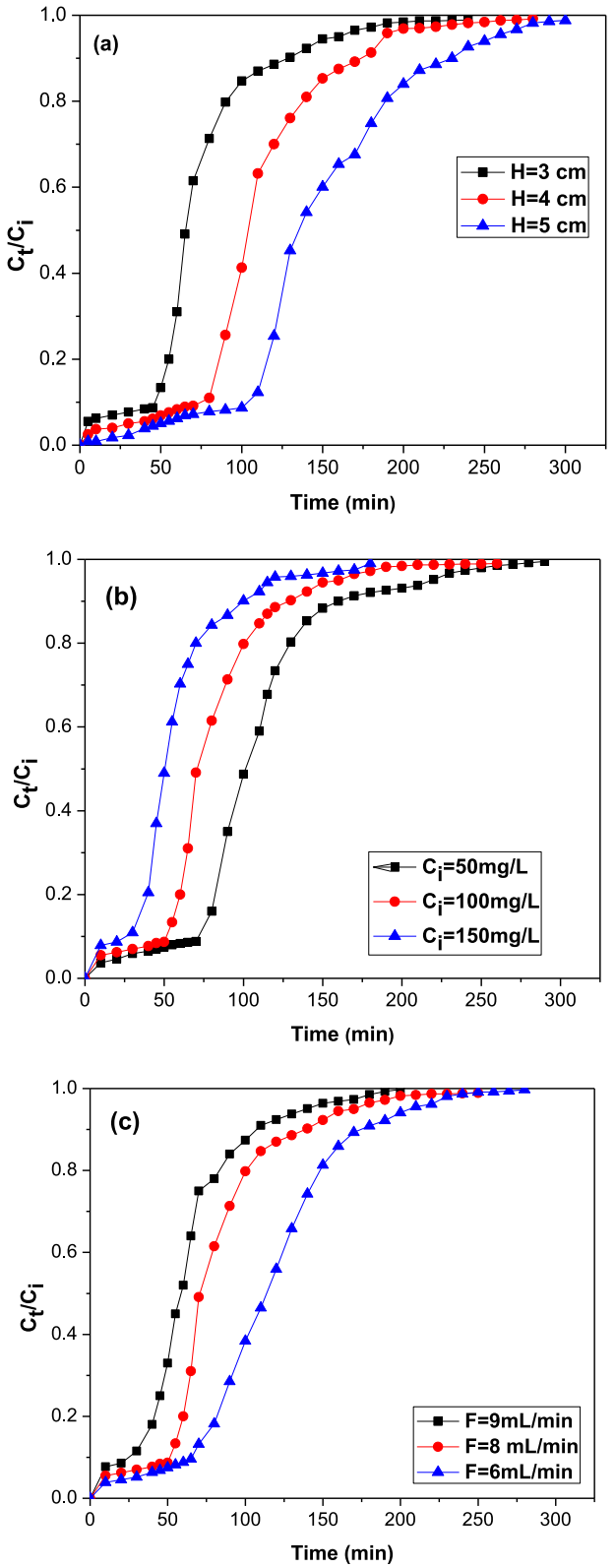

Fig. 9. Effect of operating parameters on breakthrough curve for adsorption of 3AP on SBAC adsorbent (a) effect of bed height (at constant C_i = 100 mg/L and F = 8 mL/min). (b) Effect of initial concentration (at constant, H = 3 cm and F = 8 mL/min). (c) Effect of flow rate (at constant, C_i = 100 mg/L and H = 3 cm)

Table 5
Thomas model parameters for adsorption of 3 AP using SBAC adsorbent.

H (cm)	Q (mL/min)	c_i (mg/L)	k_{Th} (mL/min mg)	q_{th} (mg/gm)	q_m (mg/g)	R^2	SSE
3	8	100	0.37	52.59	49.86	0.942	0.244
4	8	100	0.292	55.53	53.19	0.959	0.270
5	8	100	0.262	64.5	65.6	0.941	0.366
3	6	100	0.295	56.80	54.14	0.942	0.264
3	9	100	0.43	45.89	42.97	0.938	0.218
3	8	50	0.63	39.53	36.75	0.940	0.324
3	8	150	0.292	57.75	56.03	0.941	0.216

effect is that at higher concentration, substantial increase in the quantum of adsorption of 3AP is obtained as also shown in Table 4.

Jain and Gogate (2018) investigated adsorption of dye at different influent concentrations as 50 mg/L, 100 mg/L and 200 mg/L and also reported that as concentration of dye increases, the quantum of adsorption of dye increases and the time for breakthrough as well as exhaustion decreases. Han et al. (2007) also reported similar trends for adsorptive treatment of methylene blue dye on rice husk ash at different dye concentrations of 35 mg/L, 50 mg/L and 100 mg/L. It was reported that the rate of adsorption was high at higher inlet concentration of methylene blue, also yielding a decrease in breakthrough time and exhaust time.

3.3.3. Effect of 3AP solution flow rate

Adsorption study of 3AP was also performed at varying flow rates as 6 mL/min, 8 mL/min and 9 mL/min for conditions of 3 cm as height of SBAC bed and 100 mg/L as inlet concentration of 3AP solution. The obtained results given in Table 6 and Fig. 9(c) shows that by increasing the flow rate from 6 mL/min to 9 mL/min, values of breakthrough time decreased from 80 min to 30 min whereas values of exhaust time decreased from 170 min to 110 min. Due to higher 3AP flow rate, contact duration with adsorbent sites of solution decreases such that solution leaves column before equilibrium which results in lowering the uptake of 3AP on SBAC. At lesser flow rate reasonably better contact time between 3AP and SBAC was obtained which increases the extent of transfer and ultimately the adsorption of 3AP over SBAC (Seki and Yurdakoc, 2006). Similar trends can also be seen in the literature. For example, Jain and Gogate (2018) reported that, for the adsorption of acid violet 17 dye, the time for breakthrough decreased and uptake of dye decreased from 53.50 to 47.57 mg/g for changing flow rate from 6 to 10 mL/min. Vijayaraghavan et al. (2004) investigated adsorption of nickel and reported that as flow rate increases from 5 mL/min to 20 mL/min the breakthrough time and exhaust time decreased.

3.3.4. Column adsorption modelling

3.3.4.1. Thomas model. Maximum adsorption capacity during column operation can be determined using different models. Thomas model is one such model that assumes existence of plug flow in the column operation without axial dispersion and that Langmuir adsorption kinetics is followed. This model is extensively used for fixed bed adsorption study and typically observed to be suitable for adsorption operations where neither external nor internal diffusion are the limiting steps (Uddin et al., 2009). The following equation represents Thomas model. (Mathialagan and Viraraghavan, 2002)

$$\frac{c_t}{c_i} = \frac{1}{1 + \exp[\frac{K_T(mq_T - c_i V)}{\theta}]} \tag{18}$$

where, k_T is the Thomas rate constant in L / (min mg), θ is the volumetric Flow rate L/ min, m is mass of adsorbent in g in the bed and V is volume in m^3.

Linearized form of Eqs. (18) is obtained as follows (Thomas, 1944)

$$\ln(\frac{C_i}{C_t} - 1) = \frac{mk_T q_T}{\theta} - k_T c_i t \tag{19}$$

where, c_i and c_t (mg/L) are the inlet and outlet concentration of 3AP solution respectively.

Thomas model was applied to the experimental data to find the k_T and q_T values as depicted in Fig. 10(a) and the obtained values of the model parameters are represented in Table 5. It can be seen from the obtained values as the bed height of SBAC and influent concentration of 3AP increases, the q_T values and the extent of adsorption of 3AP increases though the values of k_T decrease. Similarly, with an increase in the flow rate q_T values decreases and values of k_T increase. At higher concentrations, q_T values are higher because of increase in the adsorption driving force. The values obtained for Thomas model showed that higher concentration of 3AP, higher SBAC height‘ in column and lower influent flow rate of 3AP are the favourable conditions for adsorption of 3AP on SBAC. Jain and Gogate (2018) also reported similar trend for adsorption of acid violet 17 dye whereas Han et al. (2007) illustrated similar observations for adsorption of methylene blue on rice husk ash.

The calculated values using the fitted model parameters for Thomas model and values obtained on the basis of experimental work for different SBAC bed height, flowrate and concentration are found to be very much close as shown

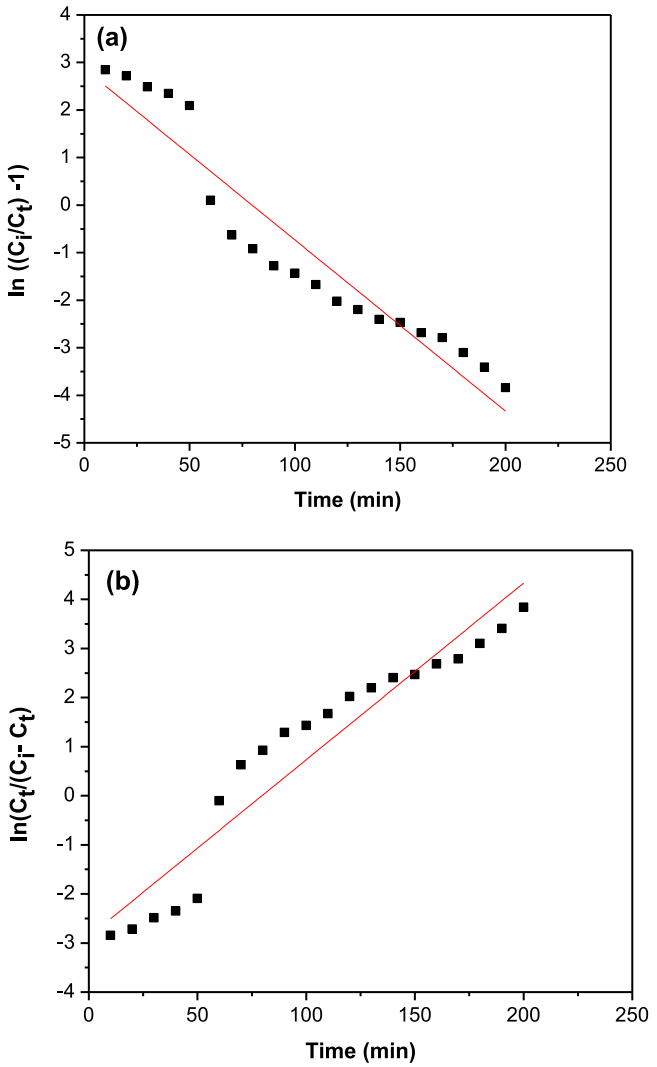

Fig. 10. (a) Thomas model and (b) Yoon–Nelson model plots for adsorption of 3AP on SBAC in column mode of operation (bed height of 3 cm, C_i = 100 mg/L and F = 8mL/min).

Table 6
Yoon–Nelson parameter for adsorption of 3 AP using SBAC adsorbent.

H (cm)	Q (mL/min)	C_i (mg/L)	k_{yN}	τ (min)	$t_{0.5}$ (min)	q (mg/gm)	R^2
3	8	100	0.037	74.67	69.12	53.3	0.942
4	8	100	0.0292	102.73	97.1	55.48	0.959
5	8	100	0.0262	146.42	140	67.26	0.941
3	6	100	0.0395	99.30	90.5	54.3	0.942
3	9	100	0.043	56.66	52.2	46.9	0.938
3	8	50	0.0325	106	100	40	0.940
3	8	150	0.0438	52.60	49.5	59.4	0.941

in Table 5. The obtained R^2 values are nearer to 0.95 for all the parameters as shown in Table 5. The error analysis was also performed using the sum of square error (SSE) analysis using following equation (Han et al., 2009)

$$SSE = \frac{\sum\left[\left(\frac{c_t}{c_i}\right) - \left(\frac{c_t}{c_i}\right)\right]^2}{n} \tag{20}$$

Table 7
Maximum adsorption capacity for removal of Pyridine and its derivatives using different adsorbents.

Pyridine andIts derivative	Adsorbent	q_{max} (mg/g)	Reference
3-Aminopyridine	Sugarcane Bagasse activated carbon	54.4	Present work
Pyridine	Bagasse fly ash	22.8	Lataye et al. (2006)
Pyridine	Rich husk ash	11.52	Lataye et al. (2008)
2-Methylpyridine	Bagasse fly ash	30.1	Lataye et al. (2008)
4-Methyl pyridine	Bagasse fly ashRich husk ash	55.216.5	Lataye et al. (2009)
2-Methyl pyridine	Agro coal ash	36	Daware et al. (2014)
2-Aminopyridine 3-Aminopyridine 4-Aminopyridine	Cobalt ferrocyanide	4.2 26.6 11.8	Alam and Kamaluddin (2000b)

As shown in Table 5, the SSE values are very less, nearer to 0.2 for all parameters. All these results established the suitability of Thomas model for adsorption of 3AP using SBAC.

3.3.4.2. Yoon–Nelson model. Yoon–Nelson model typically does not require complete data like adsorbent type, adsorbate characteristics and adsorption bed properties. Yoon–Nelson model assumes that the rate of decrease in the probability of adsorption of each molecule of pollutant is proportional to the likelihood of adsorbate adsorption and the probability of adsorbate breakthrough on the adsorbent (Han et al., 2009). The model is represented by following equations. Eq. (21) is the actual model equation and Eq. (22) is the linearized form (Baral et al., 2009)

$$\frac{c_t}{c_i} = \frac{1}{1 + \exp[k_Y\,(\tau - \mathrm{t})]} \tag{21}$$

$$\ln \frac{c_t}{c_i - c_t} = \tau k_Y - t k_Y \tag{22}$$

where, k_Y is the rate constant (min^{-1}) and τ is time (min) necessary to achieve fifty percent breakthrough. c_i and c_t (mg/L) are the inlet and outlet concentration of 3AP solution respectively and t is time. Values of k_Y and τ were estimated by plotting the graph of $\ln \frac{c_t}{c_i - c_t}$ vs. t as represented in Fig. 10(b). The obtained values of τ for Yoon–Nelson model were observed to be close to the time necessary to attain 50% breakthrough established experimentally ($t_{0.5}$). Values of all parameters at different operating conditions are summarized in Table 6. The obtained R^2 values are also nearer to 0.95 for all the fitting as shown in Table 6.

It was observed that as SBAC bed height increases, the values of k_Y decreases while the values of τ and $t_{0.5}$ increase. As the amount of SBAC increased the time of contact increased and time to reach 50% breakthrough also increased. Similarly as the influent 3AP concentration increased, the τ values decreased establishing that bed saturation takes places rapidly. With an increase in flow rate, τ was observed to decrease and k_Y increased. Results obtained in current study are similar to the results reported by Calero et al. (2009) for removal of Cr (III) by using bioadsorbent. Jain and Gogate (2018) also reported same kind of observations for adsorption of acid dye. The value of adsorption capacity for Yoon and Nelson model can be calculated using following equation (Lin and Wang, 2002)

$$q_e = c_i \theta \tau \tag{23}$$

where $q_e$is adsorption capacity of column, inlet concentration is c_i and θ is volumetric flow rate (m^3/min).

Values of adsorption capacity as obtained at different operating experimental conditions are summarized in Table 6. It was observed that the values of adsorption capacity calculated using Eq. (23) and experimentally determined are very close as shown in Table 6. All these results demonstrate suitability of Yoon–Nelson model for explaining adsorption of 3AP by SBAC.

4. Comparison of adsorption efficacy with literature

Table 7 displays the comparison of the obtained adsorption results with those represented in the literature. As the studies for pyridine derivatives were only for batch mode of operation, the comparison has also been restricted to batch studies. It can be seen from the table that the obtained value of adsorption capacity as 54.4 mg/g is comparable with two studies (only one study reported much higher adsorption capacity for saw dust based adsorbent) and mostly higher as compared with the other efforts in the literature. The comparison enables establishing good efficiency for the adsorbent synthesized in the current work.

5. Conclusions

In the current work, the efficient synthesis of SBAC adsorbent and its capability for the removal of 3 AP from wastewater have been demonstrated. Maximum removal of 3AP was obtained as 97.6% under the optimized set of conditions (pH of

6.5, SBAC dose as 6 g/L, contact time of 300 min and temperature as 303 K) with a maximum adsorption capacity as 54.4 mg/g observed for batch operation. Adsorption of 3AP was demonstrated to follow second order kinetics based on the fitting of data obtained from experimental work and error analysis using MPSD and ASE approaches. Similar analysis for different isotherm models also confirmed better fitting of Langmuir and Freundlich adsorption isotherms. Thermodynamic calculations for removal of 3AP established that adsorption is endothermic and also negative value of ΔG^0 confirmed the feasibility of adsorption mechanism. Regeneration of SBAC was also studied in presence of several eluents and it was demonstrated that maximum elution of 3AP was observed in ethanol. The column experiments performed at different initial concentrations, SBAC height and flow rate allowed establishing the best operating conditions (SBAC bed height of 5 cm, initial concentration of 3AP as 100 mg/L and flow rate of 8 mL/min) where highest adsorption efficiency was obtained as 65.66 mg/g. Thomas and Yoon–Nelson model were applied to evaluate the breakthrough parameters with demonstrated good fitting. Overall, evaluation of the capability of SBAC for adsorption of 3AP in both batch and column operations established the good efficiency of the SBAC for removal of 3AP from wastewater also establishing the important data in terms of kinetics, thermodynamics and breakthrough parameters required for design of large scale adsorption equipment.

CRediT authorship contribution statement

Gaurav B. Daware: Methodology, Investigation, Writing - original draft. **Parag R. Gogate:** Conceptualization, Supervision, Writing - review & editing, Project administration.

Declaration of competing interest

The authors declare that they have no known competing financial interests or personal relationships that could have appeared to influence the work reported in this paper.

Acknowledgement

Authors are very much thankful and also like to express their sincere gratitude to University Grants Commission, New Delhi, India for support to research under the scheme of Networking Resource Centre in Chemical Engineering at Institute of Chemical Technology, Mumbai.

Appendix A. Supplementary data

Supplementary material related to this article can be found online at https://doi.org/10.1016/j.eti.2020.100921.

References

Adib, M.R.M., Attahirah, H.M.N., Amirza, A.R.M., 2018. Phosphoric acid activation of sugarcane bagasse for removal of o-toluidine and benzidine. IOP Conf. Ser. Earth and Environ. Sci. 140, 012–029.
Alam, T., Kamaluddin, 2000a. Interaction of 2-amino, 3-amino and 4-aminopyridines with chromium and Manganese Ferro cyanides. J. Colloid Interface Sci. 224, 133–139.
Alam, T., Kamaluddin, 2000b. Interaction of 2-amino, 3-amino and 4-aminopyridines with nickel and cobalt Ferro cyanides. Physicochem. Eng. Aspects 162, 89–97.
Alonso-Davila, P., Torres-Rivera, O.L., Leyva-Ramos, R., Ocampo-Perez, R., 2012. Removal of pyridine from aqueous solution by adsorption on an activated carbon cloth. Clean Soil Air Water 40, 45–53.
Amin, N.K., 2008. Removal of reactive dye from aqueous solutions by adsorption onto activated carbons prepared from sugarcane bagasse pith. Desalination 223, 152–161.
Anoop, K.K., Anirudhan, T.S., 2002. Uptake of heavy metals in batch systems by sulfurized steam activated carbon prepared from sugarcane bagasse pith. Ind. Eng. Chem. Res. 41, 5085–5093.
Bag, B.C., Sai, M., Krishnamurti, S., Bhattacharya, C., 2009. Treatment of wastewater containing pyridine released from N, N'- Dichlorobis (2, 4, 6-trichlorophenyl) urea (CC2) plant by advanced oxidation. J. Environ. Prot. Sci. 3, 34–40.
Bageru, A.B., Srivatav, V.C., 2018. Efficient teff-straw based bio composites with chitosan and alginate for pyridine removal. Int. J. Environ. Sci. Technol. 15, 1–10.
Bai, Y., Sun, Q., Zhao, C., Wen, D., Tang, X., 2009. Aerobic degradation of pyridine by a new bacterial strain, ShinellaZoogloeoides BC026. J. Ind. Microb. Biotechnol. 36, 1391–1400.
Baral, S.S., Das, N., Ramulu, T.S., Sahoo, S.K., Das, S.N., Chaudhury, G.R., 2009. Removal of Cr (VI) by thermally activated weed *Salvinia cucullata* in a fixed-bed column. J. Hazard. Mater. 161, 1427–1435.
Belaid, K.D., Kacha, S.M., Kameche, Z., Derriche, 2013. Adsorption kinetics of some textile dyes onto granular activated carbon. J. Environ. Chem. Eng. 1, 496–503.
Blanchard, G., Maunaye, M., Martin, G., 1984. Removal of heavy metals from water by means of natural zeolites. Water Res. 18, 1501–1507.
Calero, M., Hernáinz, F., Blázquez, G., Tenorio, G., Martín-Lara, M.A., 2009. Study of Cr (III) biosorption in a fixed-bed column. J. Hazard. Mater. 171, 886–893.
Daware, G.B., Gogate, P.R., 2020. Sonochemical degradation of 3-methylpyridine (3MP) intensified using combination with various oxidants. Ultrason. Sonochem. 67, 105–120.
Daware, G.B., Vijay Babu, P.V., Pangarker, B.L., 2014. Adsorption of 2-picoline from wastewater by agro coal ash: parametric, kinetic, equilibrium and thermodynamic features. Desalination Water Treat. 52, 6263–6270.
Elsayed, M.A., 2015. Ultrasonic removal of pyridine from wastewater: optimization of the operating conditions. Appl. Water Sci. 5, 221–227.

Faki, A., Turan, M., Ozdemir, O., Turan, A.Z., 2008. Analysis of fixed bed column adsorption of reactive yellow 176 onto surfactant-modified zeolite. Ind. Eng. Chem. Res. 47, 6999–7004.
Freundlich, H.M.F., 1906. Over the adsorption in solution. J. Phys. Chem. 57, 385–470.
Gautam, R.K., Mudhoo, A., Chattopadhyaya, M.C., 2013. Kinetic, equilibrium, thermodynamic studies and spectroscopic analysis of Alizarin Red S removal by mustard husk. J. Environ. Chem. Eng. 1, 1283–1291.
Goel, J., Kadirvelu, K., Rajagopal, C., Garg, V., 2005. Removal of lead (II) by adsorption using treated granular activated carbon: Batch and column studies. J. Hazard. Mater. B125, 211–220.
Han, R., Wang, Y., Yu, W., Zou, W., Shi, J., Liu, H., 2007. Biosorption of methylene blue from aqueous solution by rice husk in a fixed-bed column. J. Hazard. Mater. 141, 713–718.
Han, R., Wang, Y., Zhao, X., Wang, Y., Xie, F., Cheng, J., Tang, M., 2009. Adsorption of methylene blue by phoenix tree leaf powder in a fixed-bed column. Experiments and prediction of breakthrough curves. Desalination 245, 284–297.
Hashemian, S., Mirshamsi, M., 2012. Kinetic and thermodynamic of adsorption of 2-picoline by sawdust from aqueous solution. J. Ind. Eng. Chem. 18, 2010–2015.
Hashemian, S., Parsaei, Y., 2015. Adsorption of 2-picoline and 3-Amino-2-picoline onto Kaolin and Organo-modified Kaolin. Orient. J. Chem. 31, 177–184.
Jain, M., Garg, V.K., Kadirvelu, K., 2010. Adsorption of hexavalent chromium from aqueous medium onto carbonaceous adsorbents prepared from waste biomass. J. Environ. Manag. 91, 949–957.
Jain, S.N., Gogate, P.R., 2017a. Acid Blue 113 removal from aqueous solution using novel biosorbent based on NaOH treated and surfactant modified fallen leaves of *Prunus Dulcis*. J. Environ. Chem. Eng. 5, 3384–3394.
Jain, S.N., Gogate, P.R., 2017b. Adsorptive removal of acid violet 17 dye from wastewater using bio sorbent obtained from NaOH and H_2SO_4 activation of fallen leaves of *Ficus racemosa*. J. Mol. Liq. 243, 132–143.
Jain, S.N., Gogate, P.R., 2018. Efficient removal of acid green dye from waste water using activated *Prunus Dulcis* as adsorbent: Batch and column study. J. Environ. Manag. 210, 226–238.
Jain, A.K., Gupta, V.K., Jain, S.S., 2004. Removal of Chlorophenols using Industrial water. Environ. Sci. Technol. 38, 1195–1200.
Jia, Z., Li, Z., Ni, T., Li, S., 2017. Adsorption of low cost absorption material based on biomass (*Corteaderia selloana* flower spikes) for dye removal: kinetics, isotherms and thermodynamics studies. J. Mol. Liq. 229, 285–292.
Kapoor, A.R., Yang, T., 1989. Correlation of equilibrium adsorption data of condensable vapours on porous adsorbents. Gas Sep. Purif. 3, 187–192.
Karale, R.S., Manu, B., Shrihari, S., 2014. Fenton and photo-fenton oxidation processes for degradation of 3-aminopyridine from water. APCBEE Proced. 9, 25–29.
Langmuir, I., 1947. The adsorption of gases on plane surfaces of glass, mica and platinum. J. Am. Chem. Zentr. 1, 875.
Lataye, D.H., Mishra, I.M., Mall, I.D., 2006. Removal of pyridine from aqueous solution by adsorption on bagasse fly Ash. Ind. Eng. Chem. Res. 45, 3934–3943.
Lataye, D.H., Mishra, I.M., Mall, I.D., 2008. Adsorption of 2-picoline onto bagasse fly ash from aqueous solution. Chem. Eng. J. 138, 35–46.
Lataye, D.H., Mishra, I.M., Mall, I.D., 2009. Adsorption of α-picoline onto rice husk ash and granular activated carbon from aqueous solution: Equilibrium and thermodynamic study. Chem. Eng. J. 147, 139–149.
Lataye, D.H., Mishra, I.M., Mall, I.D., 2011. Removal of 4-picoline from aqueous solution by adsorption onto bagasse fly ash and rice husk ash: Equilibrium. thermodynamic, and desorption study. J. Environ. Eng. 137, 1048–1057.
Lin, S.H., Wang, C.S., 2002. Treatment of high-strength phenolic wastewater by a new two-step method. J. Hazard. Mater. 90, 205–216.
Makrigianni, V., Giannakas, A., Deligiannakis, Y., Konstantinou, I., 2015. Adsorption of phenol and methylene blue from aqueous solutions by 2 pyrolytic tire char: Equilibrium and kinetic studies. J. Environ. Chem. Eng. 542, 1–9.
Mane, V.S., Mall, I.D., Srivastava, V.C., 2007. Kinetic and equilibrium isotherm studies for the adsorptive removal of Brilliant Green dye from aqueous solution by rice husk ash. J. Environ. Manag. 84, 390–400.
Marquardt, D.W., 1963. An algorithm for least-squares estimation of nonlinear parameters. J. Soc. (Ind.) Appl. Math. 11, 431–441.
Mathialagan, T., Viraraghavan, T., 2002. Adsorption of cadmium from aqueous solutions, by perlite. J. Hazard. Mater. 94, 291–303.
Mohan, D., Singh, P., Ghosh, D., 2004. Removal of pyridine from aqueous solution using low cost activated carbons derived from agricultural waste materials. Carbon 42, 2409–2421.
Mohan, D., Singh, P., Ghosh, D., 2005. Removal of α-Picoline, β-Picoline, and γ-Picoline from synthetic wastewater using low cost Activated Carbons Derived from Coconut Shell Fibers. Environ. Sci. Technol. 39, 5076–5086.
Ozturk, N., Kavak, D., 2005. Adsorption of boron from aqueous solutions using fly ash: Batch and Column studies. J. Hazard. Mater. B 127, 81–88.
Padoley, K.V., Mudliar, S.N., Banerjee, S.K., Deshmukh, S.C., Pandey, R.A., 2011. Fenton oxidation: A pre-treatment option for improved biological treatment of pyridine and 3-cyanopyridine plant wastewater. Chem. Eng. J. 166, 1–9.
Ramavandi, B., Farjadfard, S., Ardjmand, M., 2014. Mitigation of orange II dye from simulated and actual wastewater using bimetallic chitosan particles: Continuous flow fixed-bed reactor. J. Environ. Chem. Eng. 2, 1776–1784.
Reddy, M.D., Reddy, G., 2012. Microbial degradation of Pyridine and its derivatives. In: Microorganism in Environ. Manag.. pp. 249–262, Book Chapter.
Sadaf, S., Bhatti, H.N., Nausheen, S., Amin, M., 2015. Application of a novel lignocellulosic biomaterial for the removal of Direct Yellow 50 dye from aqueous solution: Batch and column study. J. Taiwan Inst. Chem. Eng. 47, 160–170.
Seki, Y., Yurdakoc, K., 2006. Adsorption of promethazine hydrochloride with KSF montmorillonite. J. Mater. Sci. 12, 89–100.
Singh, K., Chandra, B., Rhyman, L., Ramasami, P., 2016a. Effective adsorption of pyridine (Py) onto mesoporous silica derived from de-oiled mustard cake (DOMC): Experimental and theoretical study. J. Environ. Chem. Eng. 4, 1383–1392.
Singh, D.K., Kumar, V., Mohan, S., Hasan, D.S., Hasan, H., 2016b. Breakthrough curve modelling of grapheme oxide aerogel packed fixed-bed column for the removal of cr (VI) from water. J. Water Proc. Eng. 18, 150–158.
Stern, M., Elmar, H., Kut, O., Hungerbbuhler, K., 1997. Removal of substituted pyridines by combined Ozonation/fluidized bed biofilm treatment. Water Sci. Technol. 35, 329–335.
Temkin, M.I., Pyzhev, V., 1940. Kinetics of ammonia synthesis on promoted iron catalyst. Acta Phys. Chem. URSS 12, 327–356.
Thomas, H.C., 1944. Heterogeneous ion exchange in a flowing system. J. Am. Chem. Soc. 66, 1664–1666.
Uddin, Md.T., Rukanuzzaman, Md., Khan, M.R., Islam, Md.A., 2009. Adsorption of methylene blue from aqueous solution by jackfruit leaf powder: A fixed-bed column study. J. Envion. Manag. 90, 3443–3450.
Vijayaraghavan, K., Jegan, J., Palanivelu, K., Velan, M., 2004. Removal of nickel (II) ions from aqueous solution using crab shell particles in a packed bed up-flow column. J. Hazard. Mater. B 113, 223–230.
Weber, W.J., Morris, J.C., 1963. Kinetics of adsorption on carbon from solution. J. Sanit. Eng. Div. Am. Soc. IV Eng. 89, 31–60.
Xia, M., Jin, C., Kong, X., Jiang, M., Lei, D., Lei, X., 2018. Green removal of pyridine from water via adsolubilization with lignosulfonate intercalated layered double hydroxide. Adsorpt. Sci. Technol. 36, 982–998.
Zalat, O.A., Elsayed, M.A., 2013. A study on microwave removal of pyridine from wastewater. J. Environ. Chem. Eng. 1, 137–143.
Zhang, C., Li, M., Luo, L.H., Zhang, R., 2009. Pyridine degradation in the microbial fuel cells. J. Hazard. Mater. 172, 465–471.
Zhao, H., Xu, S., Zhong, J., Bao, X., 2004. Kinetic study on the photo-catalytic degradation of pyridine in TiO_2 suspension systems. Catalysis 3, 857–861.